Bioinformatics, 31(7), 2015, 1053–1059
doi: 10.1093/bioinformatics/btu776
Advance Access Publication Date: 25 November 2014
Original Paper

OXFORD

Systems biology

Mechanotransduction map: simulation model, molecular pathway, gene set

Jennifer E. Dent[1,2,†], Valentina Devescovi[1,†], Han Li[1,†], Pietro Di Lena[3], Youtao Lu[1], Yuanhua Liu[1] and Christine Nardini[1,*]

[1]Group of Clinical Genomic Networks, Key Laboratory of Computational Biology, CAS-MPG Partner Institute for Computational Biology, Shanghai Institutes for Biological Sciences, Shanghai, People's Republic of China, [2]Quintiles, Global Biostatistics, Reading, Berkshire, UK and [3]Department of Computer Science and Engineering - DISI, University of Bologna, Bologna, Italy

†The authors wish it to be known that, in their opinion, the first three authors should be regarded as Joint First Authors.
*To whom correspondence should be addressed.
Associate Editor: Igor Jurisica

Received on May 30, 2014; revised on October 30, 2014; accepted on November 17, 2014

Abstract

Motivation: Mechanotransduction—the ability to output a biochemical signal from a mechanical input—is related to the initiation and progression of a broad spectrum of molecular events. Yet, the characterization of mechanotransduction lacks some of the most basic tools as, for instance, it can hardly be recognized by enrichment analysis tools, nor could we find any pathway representation. This greatly limits computational testing and hypothesis generation on mechanotransduction biological relevance and involvement in disease or physiological mechanisms.
Results: We here present a molecular map of mechanotransduction, built in CellDesigner to warrant that maximum information is embedded in a compact network format. To validate the map's necessity we tested its redundancy in comparison with existing pathways, and to estimate its sufficiency, we quantified its ability to reproduce biological events with dynamic simulations, using Signaling Petri Networks.
Availability and implementation: SMBL language map is available in the Supplementary Data: core_map.xml, basic_map.xml.
Contact: christine.nardini.rsrc@gmail.com
Supplementary information: Supplementary data are available at *Bioinformatics* online.

1 Introduction

Mechanotransduction is a ubiquitous phenomenon, the importance and complexity of which has not yet been fully captured. Yet, mechanical stresses are triggers for wound healing (Cordeiro and Jacinto, 2013) and can initiate epithelial-mesenchymal transition (EMT) in the presence of inflammation (Gomez *et al.*, 2010). Both these phenomena are tightly related and important in the understanding of broader events like development (EMT Type 1), tissue regeneration/healing (EMT Type 2) and tumorigenesis (EMT Type 3) (Kalluri, 2009; Kalluri and Weinberg, 2009). Therefore, the understanding of these events for applications in regenerative and cancer medicine (Roussos *et al.*, 2010), as well as in the treatment of inflammatory and autoimmune diseases (González *et al.*, 2011; Lu *et al.*, 2006; Schäfer and Werner, 2008), is of crucial importance. In addition, given the possibility to induce mechanical stimuli in a relatively ample number of (accidental) ways (Hattori *et al.*, 2009; Pecchi *et al.*, 2014), understanding the extent of the phenomenon acquires practical relevance in numerous clinical areas.

We observed, however, that, despite its importance, mechanotransduction is poorly represented in terms of pathways and molecular maps, which are nevertheless crucial tools when medical research is performed in the frame of omic studies as it is the case for a growing number of maladies, trying to unravel the complexity of chronic inflammatory autoimmune diseases and cancers (Shen *et al.*, 2009;

Wu *et al.*, 2010). For this reason, we reconstructed the molecular map of mechanotransduction using approved standard (Hucka *et al.*, 2003, 2004) which allows a detailed and yet compact description of the relations ongoing among molecules, easy sharing and editing of the map as well as topological analysis (Bonnet *et al.*, 2013; Smoot *et al.*, 2011) and dynamic simulations (Dent *et al.*, 2013; Theocharidis *et al.*, 2009).

Having built this map we were able to better quantify its overlap (Dent *et al.*, 2013; Di Lena *et al.*, 2013) with known pathways in Reactome (Croft *et al.*, 2011) and Panther (Mi *et al.*, 2005). The non-statistically significant overlaps with the pathways in these two databases imply minimum redundancy, confirming the need for a mechanotransduction pathway representation. We then validated the map's ability to reproduce known information by dynamic simulations mimicking published experimental settings (Gomez *et al.*, 2010; Langevin *et al.*, 2006). Given the successful tests run on the map's ability to mimic the effects of mechanical stress in relation to inflammation, relevant for example in rheumatic diseases, this network becomes an appropriate and flexible tool for the preliminary investigation *in silico* of therapeutic alternatives and side effects of mechanical stresses in inflammation-related contexts.

2 Results

2.1 Map necessity

A mechanotransduction map was built with the species (genes, transcripts, proteins, listed in SupplementaryInfo1 Table S1) collected from 15 high-quality publications reported in SupplementaryInfo1 Table S2 (Chalfie, 2009; Chiquet *et al.*, 2009; Dupont *et al.*, 2011; Farge, 2003; Gomez *et al.*, 2010; Hoffman *et al.*, 2011; Ingber, 2006; Langevin *et al.*, 2006; Marshall and Lumpkin, 2012; Mendez and Janmey, 2012; Schwarz and Gardel, 2012; Somogyi and Rørth, 2004; Wall and Banes, 2005; Zebda *et al.*, 2012; Zhang and Labouesse, 2012) manually curated and reported in the CellDesigner standard (Hucka *et al.*, 2004). The map comes in two versions both available at http://www.picb.ac.cn/ClinicalGenomicNTW/Mechanotransduction.html, one named *core*, built exclusively from literature, collecting 67 species and 47 reactions (Fig. 1A) and one named *basic*, which includes extensions from KEGG pathways (Kanehisa and Goto, 2000) increasing the size to 234 species and 245 reactions.

The maps were initially tested with MIMO (Di Lena *et al.*, 2013) to assess the maps' necessity in terms of redundancy with publicly available CellDesigner pathways, and namely Reactome (Croft *et al.*, 2011) and Panther (Croft *et al.*, 2011). This type of test builds on classical enrichment analyses which are typically assessed by taking into account the amount of common molecules in two pathways. MIMO, however, adds to this the analysis at the reaction level, to keep into account the way in which molecules interact. Our results indicate that the overlap is limited, i.e. non-statistically significant, nor biologically relevant.

In fact, at the molecular level, the overlap (Fig. 1B, Table 1 and SupplementaryInfo1 Tables S3–S5, column 2) concerns a very limited and scattered number of extra to intraintracellular signal effectors such as extracellular Ca^{2+} intake and activation at the cell membrane level of phospholipases C, beta (PLCβ 1-4), an important player in the initiation of mechano-mediated and receptor-mediated signal transduction by generation of second messengers like inositol 1,4,5-trisphosphate (IP3). The transduction of the mechanical stimulus is next embodied directly in the cytosol in the RHOs family (RAC1, CDC42) and the actin protein filaments (F-actin).

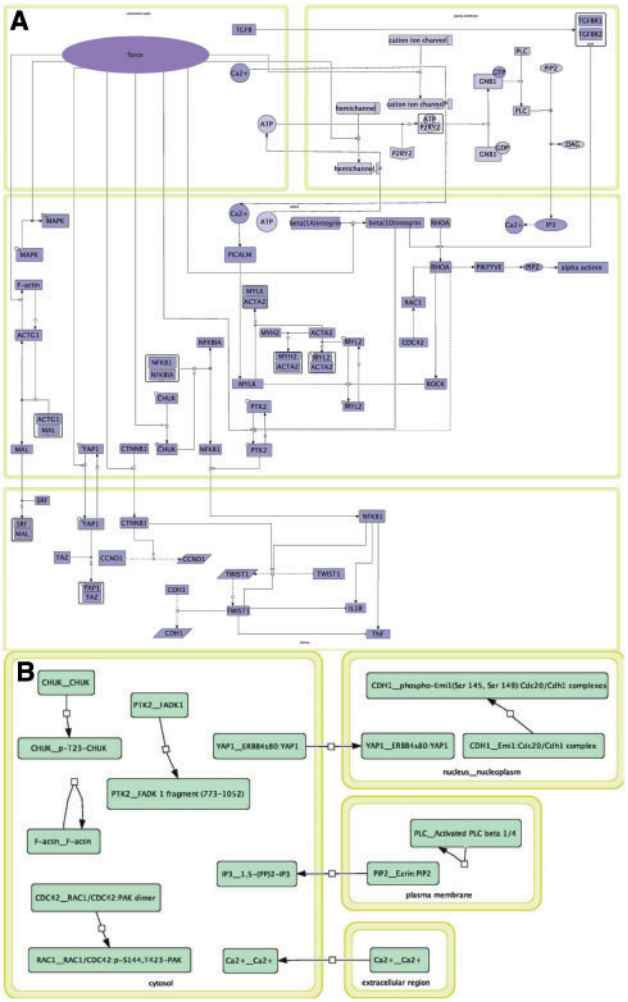

Fig. 1. (**A**) Snapshot of the reconstructed Celldesigner mechanotransduction map, including 67 species and 47 reactions (the SMBL file is available at http://www.picb.ac.cn/ClinicalGenomicNTW/Mechanotransduction.html). (**B**) Overlap between the mechanotransduction map and the whole human set of Reactome pathways (Croft *et al.*, 2011), processed by MIMO (Di Lena *et al.*, 2013). The names of the mapped molecules are separated by a double underscore (__), where the first portion refers to the mechanotransduction map and the second to the whole human Reactome map. The emerging overlaps are extremely fragmented and concern extracellular Ca^{2+} intake, activation of phospholipases C, beta 1-4 (PLCβ 1-4) signaling and generation of cytosolic inositol 3P as consequence. Mechanotransduction typical signals like RHOs family (e.g. RAC1, CDC42) activities and cytoskeletal structural protein actin filaments (F-actin) are interested at the cytosol level, whereas cell-to-cell adhesion molecules (cadherins) emerge in the nucleus

Finally, EMT-related molecules appear in the nucleus, marked by the epithelial adhesive cadherins. Even when extending the map (i.e. *basic* map) the number of overlapping molecules only slightly increases (SupplementaryInfo1 Tables S4–S5, column 2).

When shifting from the overlapping molecules to the overlapping pathways, Immune System, Inflammation and several downstream-specific signal transductions represent a higher amount of matching, but still involving only a few molecules and reactions from the *core*/*basic* maps (see Table 1 and SupplementaryInfo1 Tables S3–S5, column 3). This overlap, not significant, nevertheless indicates where the connection of the effects of mechanical stimulation to inflammatory conditions occurs, i.e. at one subunit of the master kinase for

Table 1. Ranked reactome pathways overlapping with the mechanotransduction *core* map

Pathway name	Overlap score	#Matched molecules	#Matched reactions
Immune system	0.0496	6	3
Innate immune system	0.0496	6	3
Adaptive immune system	0.0496	6	3
Developmental biology	0.0390	3	2
Axon guidance	0.0390	3	2
Downstream signal transduction	0.0355	5	3
Signaling by PDGF	0.0355	5	3
Signaling by GPCR	0.0355	4	2
GPCR downstream signaling	0.0355	4	2
Hemostasis	0.0355	4	2
Fcgamma receptor-dependent phagocytosis	0.0355	4	2
Apoptotic execution phase	0.0355	4	2
Apoptotic cleavage of cellular proteins	0.0355	4	2
Apoptosis	0.0355	4	2
Signaling by NGF	0.0284	4	2
NGF signaling via TRKA from the plasma membrane	0.0284	4	2
DAP12 signaling	0.0284	4	2
DAP12 interactions	0.0284	4	2
Signaling by the B cell Receptor (BCR)	0.0284	4	2
Signaling by ERBB4	0.0284	4	2
Signaling by ERBB2	0.0284	4	2
Signaling by EGFR in cancer	0.0284	4	2
Signaling by EGFR	0.0284	4	2
PLC beta mediated events	0.0213	3	2
Opioid signaling	0.0213	3	2
G-protein mediated events	0.0213	3	2

MIMO-detected hits were filtered by removing those involving less than three molecules or less than three reactions. Overlap between two pathways is quantified by counting the respective fraction of matched reactions. A weight is assigned to every matched reaction depending on the number of matched molecules that take part to the reaction. The Overlap score [0,1] gives an estimation of how much the query pathway (mechanotransduction *core*) is contained into the target pathway (Reactome pathways). The largest overlaps, Mechanotransduction *core* versus Immune System pathway, involve only 6 out of 65 species and 3 out of 47 reactions.

NF-κB activation (nuclear factor of kappa light polypeptide gene enhancer in B-cells 1), namely conserved helix-loop-helix ubiquitous kinase, and the NF-κB inducible factor protein tyrosine kinase 2, see *basic* map with Reactome overlap (SupplementaryInfo1 Table S4, column 3).

Globally, both molecules and pathways comparison analyses outline a lack of information about mechanotransduction as a defined signaling network in the two public databases.

2.2 Map sufficiency

The map was then tested for its sufficiency, i.e. usability in (re)producing biological phenomena triggered by mechanical stimulations, with the aim of validating the map's usage in relation to open problems where the impact of mechanical stresses is of relevance, as it is the case in arthritic diseases (Croft *et al.*, 2011; Hattori *et al.*, 2009). We therefore compared the effects of a mechanical stimulation on the molecules involved in our network, over time and under different inflammatory conditions. The experimental gold standard to validate the results was chosen from two articles (Gomez *et al.*, 2010; Langevin *et al.*, 2006) that explore diverse effects in similar, i.e. comparable, settings (mouse tissue). Jointly, the experimental set ups indicate, as effects of the mechanical stimulation in healthy tissue, the activation of RhoA/Rac1 (ras homolog family member A/rho family, small GTP binding protein Rac1) and actomyosin, and the presence of EMT, accompanied by the (early) activation of myocardin-related transcription factors (MRTF-A/MKL1/MAL and MRTF-B/MKL2) unaffected by the inhibition of Rac1, in inflamed tissue.

For validation of the ability of our map to reproduce these settings, we used the Petri Network framework [Biolayout Express3D (Theocharidis *et al.*, 2009) and SPNconverter (Dent *et al.*, 2013)]. *In silico* experiments were run assuming that 100 time blocks could cover the whole simulation time, 100 tokens could represent physiological baseline genes regulation and 500 tokens could mimic upregulation, as previously reported (Dent and Nardini, 2013). Tokens' distribution as well as relevant statistics is available in SupplementaryInfo1 Tables S6–S7, evaluation of the stability of the simulations in SupplementaryInfo1 Tables S8–S10 and in Section 3. Results are presented in Figure 2 where the 'Summary' column indicates the coherence between the outcomes of the major biological events tested by our simulations in comparison to the published experiments.

More in details, the simulation referred specifically to the mechanotransduction markers (Fig. 2, rows 1–9) recapitulates the dynamics of mechanosensitive genes via pathways linked to mechanically induced cytoskeletal remodeling (Chiquet *et al.*, 2009). Namely, tissue cells subjected to tensions from the extracellular environment sense and exert forces via their cytoskeleton, which undergo reorganization in a different shape and functionality, leading to migration and cell spreading as exemplar of these temporary cell structure modifications (Ponti *et al.*, 2004; Theriot and Mitchison, 1991). In all cases the early steps of the process require the transient activity of MAL, one of SRF transcriptional cofactors, which is specifically induced by a mechanical stimulus (i.e. cell stretching) and, once activated, affects cytoskeletal actin dynamics (Posern and Treisman, 2006; Somogyi and Rørth, 2004). As indicated in the reference experiment by Langevin *et al.* (2006) the temporal sequence of events following the subconnective tissue physical stimulation resulting in active changes of fibroblasts cytoskeleton starts with the initial pulling of the extracellular matrix (ECM) on cells at precise focal adhesions complexes followed by actin rearrangement (like MAL expression induces); after focal contacts appear on cell surface stimulated by the tensile forces (Rac1 driven), RhoA activate actomyosin contraction around lamellipodia, through the stimulation of the down-stream effector Rho kinase (Rho-associated, coiled-coil containing protein kinase 1, ROCK family).

All these events are reproduced in our map, and remarkably, with the correct subtle timing they present *in vivo*: i.e. stable late activation of the Rho kinase and early transient activation of MAL.

In particular, since the whole RHOs family (RHOA; RAC1; CDC42, cell division cycle 42) action is related to mechanotransduction via its activity on actomyosin (Machacek *et al.*, 2009; Parsons *et al.*, 2010), and given that the inhibition of one only of the family members does not impede downstream events to occur (see Gomez *et al.*, 2010 for EMT occurring even with inhibition of Rac1), we mark as coherent complexes/families where one or more constituent molecules do have the expected up or downregulation, and others

CORE MAP	EXPERIMENTS	Needle-Mechanotransduction			Mechanotransduction-EMT			Summary	
		Simulation TGFβ=100		Experiment (Langevin et al, 2006)	Simulation TGFβ=500		Experiment (Gomez et al, 2010)		
		p(t-val)	Tokens (t)		*p (t-val)*	Tokens (t)			
alpha-actinin	ACTOMYOSIN	↑ (-10.03)		↑√	↑ (-11.42)		↑√	↑√	Mechanotransduction
ACTA2		- (0.86)			- (-1.25)				
MYH2		- (1.64)			- (-0.14)				
MYLK		↑ (-14.85)			↑ (-13.56)				
MYL2		- (0.00)			- (0.00)				
RHOs (RAC1, RHOA|active, CDC42)	RAC1	- (-0.64)		↑X	- (0.28)		↑X	↑√	
	RHOA	↑ (-6.56)		NA	↑ (-7.73)		NA		
	CDC42	- (0.68)		NA	- (0.63)		NA		
ROCK	ROCK	↑ (-8.64)		↑√	↑ (-8.94)		↑√	↑√	
MAPK|active	JNK-2	↑ (-16.41)		↑√	↑ (-16.83)		NA	↑√	
MAL:SRF	MAL	- (1.05)		NA	- (-0.75)		↑√*	↑√*	
TWIST1	TWIST1	↑ (-2.60)		NA	↑ (-5.01)		NA	↑√	EMT
rTWIST1								↑√	
rCDH1	rCDH1	↓ (10.34)		NA	↓ (12.56)		NA	↑√	
IL1B	IL1B	- (-1.90)		NA	↑ (-2.76)		NA	↑√	Inflamm.

Fig. 2. Molecules in column 1 belong to the reconstructed mechanotransduction map (*core*), compared with the activity observed in two experimental setting published, respectively, (Langevin *et al.*, 2006b) and (Gomez *et al.*, 2010). When the exact molecule is not shared between our map and the published results, proxies are chosen from literature. Prefix *r*, standing for RNA, indicates transcripts, while the absence of a prefix indicates proteins. The input of the simulation is the variation of the force. 'NA' indicates that the molecule was not tested in the corresponding experiment, '-' that the molecule shows no significant change upon force activation, '↑' and '↓' indicate statistically significant up and downregulation, respectively, accompanied by the *t*-values. In simulation the qualitative trend of activation of the gene is also presented with time blocks on the *x*-axis and tokens on the *y*-axis (for larger figures and details see Supplementary Fig. S1). MAL, a known early gene, bound to SRC (MAL:SRC) clearly presents the early gene pattern of activity (tokens count, *y*-axis) over 100 time blocks (*x*-axis) in simulation. Columns 5–8–9 indicate by means of ticks and crosses the agreement between the experiments and the corresponding simulation

appear unchanged. With the same rationale we considered the actomyosin complex.

2.3 Simulation relevant in autoimmunity

We then moved to test the altered condition, relevant to autoimmune diseases and injured tissues, represented by an inflamed microenvironment. In such situations both physical stresses and biochemical signals' complexities are increased, and mechanical stresses trigger wound healing where EMT occurs in cells needing to be competent (i.e. motile phenotype, cell proliferation, ECM deposition) to remodel tissue around the wound (Cordeiro and Jacinto, 2013; Gomez *et al.*, 2010). To perform this simulation we observed the behavior of markers of EMT (Fig. 2, rows 10–12): TWIST1 (twist

family bHLH transcription factor 1) and CDH1, also known as E-cadherin (Lee and Nelson, 2012), which expression is considered a clear indicator of the switch to EMT program (Kroepil *et al.*, 2012) in a computational model of tissue inflammation (100 tokens at time 0 on TGFβ).

In our results, the activation of the immediate early MAL and late RHOA/RAC1—actomyosin mechanotransduction signaling—matches with the activity of CDH1 and TWIST1 during the EM transition (i.e. up and down, respectively).

As a final test, inflammation was also monitored with the sole molecule (IL1β; interleukin 1, beta) that behaves differentially in the two simulations settings (inflamed versus non-inflamed tissue, i.e. transforming growth factor, beta, TGFβ = 100 and TGFβ = 500, respectively, Fig. 2, row 13). IL1β is an inflammatory cytokine that can stimulate the release of prostaglandin and collagenase from connective cells (i.e. synovial fibroblasts—Van Damme *et al.*, 1985), coherently up-regulated in the second setting only.In conclusion the map can describe the TGFβ-mediated EMT, and its early regulation by MAL nuclear transition and environmental mechanical forces, as previously validated in an inflammatory experimental model by Gomez *et al.* (2010). Investigating the aspects of EMT for tissue healing in inflammation is relevant in health and disease, since this process drives tissue remodeling to protect and repair injuries; yet if the transition becomes uncontrolled, like in chronic inflamed tissues, a scarring tissue overgrowth (fibrosis) happens, resulting in organ dysfunction and eventually failure (Wynn, 2008). For this reason the information on crucial signals of mechanotransduction (RHOs Family; actomyosin and catenin beta 1, CTNN1) together with EMT (CDH1, TWIST1) and inflammation (NF-κB, TGFβ and transforming growth factor beta receptor) that our map is able to gain are of great relevance for the application of mechanical stimuli as means to control EMT, the reverse phenomenon MET and to gain insight for example into treatments of tissue fibrosis, all with clinical implications in inflammatory chronic diseases, such as Arthritis and Diabetes, as well as wound healing and fibrosis (Wong *et al.*, 2012).

Overall, Figure 2 shows high coherence with the simulation results matching experimental results for four of the five tested molecules (the exception being the failure of the simulation to match experimental results for RAC1 when considered alone and not as the synergistic RHOs family) and overall coherence summarized at 100%.

3 Methods

3.1 Map construction

The map was designed based on the species listed in SupplementaryInfo1 Table S1 collected from 15 high-quality publications reported in SupplementaryInfo1 Table S2 and manually curated in CellDesigner (http://www.picb.ac.cn/ClinicalGenomicNTW/Mechanotransduction.html). Complexes were either treated as units, like ion channels and hemichannels, similarly to what is done in Reactome (REACT_160271.1, TPCN1/2 transport lysosomal Ca^{2+} to cytosol); or explicated in a literature-based selection of their components, like the actomyosin complex, based on the functionality of the complex itself. All implementative choices are detailed in SupplementaryInfo1, column *NOTES*.

For the map construction, genes (nodes) were all converted to human official gene symbols and for comparison with published experiments further converted to mouse homologues (http://www.ncbi.nlm.nih.gov/unigene/). In the text we used the human genes symbols for molecules when we referred to our results, and mouse genes symbols when we referred to published data. The maps come in two versions based on the origin of the nodes: the *core* map, contains nodes extracted exclusively from literature; the *basic* map includes nodes from KEGG pathways (Kanehisa and Goto, 2000). Such an extension was operated by using each of the core molecules as a query term in KEGG, and by adding the corresponding pathway into the *basic* map. For both maps the connections between nodes, when not explicated in literature, were based on the KEGG Orthology (KO) groups, in order to generalize evidence obtained in specific organisms to other organisms.

3.2 Map overlap

The pathway comparison analysis was performed with MIMO (Di Lena *et al.*, 2013) against the set of human pathways annotated in the Reactome (Croft *et al.*, 2011) and Panther (Mi *et al.*, 2005) repositories. The popular KEGG pathways (Kanehisa and Goto, 2000) were excluded from this analysis, since currently we did not find tools able to automatically convert in full KEGG pathways in SBML format (with the exception of the metabolic pathways). MIMO requires in input two pathways in SBML format (Hucka *et al.*, 2003, 2004), a list of allowed mappings between molecules in the two pathways and a maximum length-parameter *N*. In short, each pathway in input is spliced into a set of shortest paths, of maximum length *N*, between molecules. A shortest path simply identifies the shortest chain of reactions connecting two molecules. Two chains of reactions (one in each pathway) are considered equivalent if both molecules at their extremes can be matched, according to the list provided in input. The overlap is then obtained by detecting the largest set of equivalent chains in the two pathways. The analysis was performed with $N = 3$. The list of mappings between molecules was obtained automatically by pattern matching between the names assigned to molecules in the Mechanotransduction and Reactome/Panther pathways. Since the name identifiers adopted in Reactome are usually human-readable and non-standard, the string identifiers in Reactome were extended by including all their possible synonyms (such as standard gene/protein names). The list of names/synonyms for the participating molecules in a Reactome pathway can be obtained automatically from the Reactome website (http://www.reactome.org).

The *core* and *basic* mechanotrasduction maps were compared with the whole human map in Reactome to detect the largest possible set of common reactions. In addition, to allow an automated analysis of the biological meaning of such overlaps, enrichments on the entire collection of Reactome pathways (which constitute the whole map) was carried out at the reaction level (single reactions are identified by a unique internal ID, i.e. the same reaction in different pathways is identified by its unique ID) by performing a standard Fisher's exact test on the set of reactions highlighted in the overlap with the whole human Reactome map. The same approach could not be replicated on the Panther dataset, since Panther provides only a collection of single pathways and not a full map on human.

3.3 Simulations

The maps' input was identified in the Force (node: force@extracellular) and molecular modifications were simulated dynamically in the Signaling Petri Network frame after transforming the CellDesigner map into a compatible BiolayoutExpress3D input (Theocharidis *et al.*, 2009), using the SPNConverter plugin we recently designed (Dent *et al.*, 2013). Based on previous approaches (Dent and Nardini, 2013), we created a set of baseline conditions, where all edge nodes were assigned 100 tokens at time 0. As the simulation

model runs, and at each time point, tokens are passed through *gates* between molecules. As the number of tokens at a molecule rises and falls with time, we see a representation of, in the case of the mechanotransduction map, gene regulation and mechanical stress [e.g. an increase in the number of tokens representing upregulation and a decrease, downregulation (Ruths *et al.*, 2008)]. Over the course of the simulation, most networks will reach a stable state, where the number of tokens at nodes within the network no longer fluctuates significantly. By changing the number of tokens that a molecule is assigned at time 0, we can consider the potential effect that perturbing specific molecules may have on the map. Thus, simulation reproducing the setting in Gomez *et al.* (2010) was achieved by preserving the baseline conditions of 100 tokens at time 0 at all edge nodes, with the exception of TGFB, which was assigned 500 tokens (for simulated upregulation). The number of tokens assigned to force was then increased from 100 to 500 (SupplementaryInfo1 Table S6). Simulations reproducing the setting of Langevin *et al.* (2006) were performed with the baseline conditions preserved, and changing only the number of tokens assigned to 'force' (SupplementaryInfo1 Table S7). One hundred time points and 1000 simulations were run for each setting. Evaluation of the statistical significance of the differentially expressed genes was computed by considering the number of molecules that were significantly different at the 100th time point, compared with the baseline conditions.

To determine the statistical significance of the differentially expressed genes in the simulations the *t*-value was calculated at each time point for the baseline and perturbed distributions according to the equation:

$$t\text{-value} = \frac{\mu_{i,b} - \mu_{i,p}}{\sqrt{\frac{\sigma^2_{i,b}}{500} + \frac{\sigma^2_{i,p}}{500}}},$$

where $\mu_{i,s}$ and $\sigma^2_{i,s}$ represent the mean and variance of the number of tokens at node *i*, for the baseline (*b*) and perturbed (*p*) networks, respectively. Comparing the absolute *t*-value with the corresponding critical value ($t0.05, 1000 = 1.96$) at the 100th (and thus most stable) time point, those molecules whose expression level significantly changed in each simulation were identified.

Experiments to evaluate the stability of the simulation were performed by repeating simulations around force stimulation three times on both the *core* and *basic* maps (SupplementaryInfo1 Tables S8–S9). Results of Wilcoxon rank sum tests showed no statistical difference between simulations runs. Overlap between molecules significantly changed ($P < 0.05$) in different simulation runs lead to different levels of reproducibility (percent overlap) for the *core* (~90%) and *basic* maps (~60%) with no changes when raising the number of simulations to 5000 (SupplementaryInfo1 Table S10). For this reason, dynamic simulations were run on the *core* map only, assuming it reaches the limit size for simulations with BiolayoutExpress3D (Theocharidis *et al.*, 2009). The first set of simulation results was preserved as our reference. All statistical analyses were performed in R v2.13.0 (Ihaka and Gentleman, 1996).

Funding

This project was funded by MoST international cooperation program [no. 2013DFA30790, and NSFC n. 31070748], JED collaborated in the frame of the European Commission [FP7-PEOPLE-2011-IRSES program 31028760, project ID 294935].

Conflict of Interest: Jennifer E. Dent declares that although all work was conducted under the EU-FP7-PEOPLE-2011-IRSES program, her current (and only) affiliation is with Quintiles, which is a public company.

References

Bonnet,E. *et al.* (2013) BiNoM 2.0, a Cytoscape plugin for accessing and analyzing pathways using standard systems biology formats. *BMC Syst. Biol.*, **7**, 18.

Chalfie,M. (2009) Neurosensory mechanotransduction. *Nat. Rev. Mol. Cell Biol.*, **10**, 44–52.

Chiquet,M. *et al.* (2009) From mechanotransduction to extracellular matrix gene expression in fibroblasts. *Biochim. Biophys. Acta*, **1793**, 911–920.

Cordeiro,J.V. and Jacinto,A. (2013) The role of transcription-independent damage signals in the initiation of epithelial wound healing. *Nat. Rev. Mol. Cell Biol.*, **14**, 249–262.

Croft,D. *et al.* (2011) Reactome: a database of reactions, pathways and biological processes. *Nucleic Acids Res.*, **39**, D691–D697.

Dent,J.E. and Nardini,C. (2013) From desk to bed: computational simulations provide indication for rheumatoid arthritis clinical trials. *BMC Syst. Biol.*, **7**, 10.

Dent,J.E. *et al.* (2013) SPNConverter: a new link between static and dynamic complex network analysis. *Bioinformatics* **29**, 2507–2508.

Di Lena,P. *et al.* (2013) MIMO: an efficient tool for molecular interaction maps overlap. *BMC Bioinformatics*, **14**, 159.

Dupont,S. *et al.* (2011) Role of YAP/TAZ in mechanotransduction. *Nature*, **474**, 179–183.

Farge,E. (2003) Mechanical induction of twist in the Drosophila foregut/stomodeal primordium. *Curr. Biol.*, **13**, 1365–1377.

Gomez,E.W. *et al.* (2010) Tissue geometry patterns epithelial-mesenchymal transition via intercellular mechanotransduction. *J. Cell. Biochem.*, **110**, 44–51.

González,S. *et al.* (2011) Mechanotransduction and epigenetic control in autoimmune diseases. *Autoimmun. Rev.*, **10**, 175–179.

Hattori,K. *et al.* (2009) Mechanical effects of surgical procedures on osteochondral grafts elucidated by osmotic loading and real-time ultrasound. *Arthritis Res. Ther.*, **11**, R134.

Hoffman,B.D. *et al.* (2011) Dynamic molecular processes mediate cellular mechanotransduction. *Nature*, **475**, 316–323.

Hucka,M. *et al.* (2003) The systems biology markup language (SBML): a medium for representation and exchange of biochemical network models. *Bioinformatics*, **19**, 524–531.

Hucka,M. *et al.* (2004) Evolving a lingua franca and associated software infrastructure for computational systems biology: the Systems Biology Markup Language (SBML) project. *Syst. Biol.*, **1**, 41–53.

Ihaka,R. and Gentleman,R. (1996) R: a language for data analysis and graphics. *J. Comput. Graph. Stat.*, **5**, 299–314.

Ingber,D.E. (2006) Cellular mechanotransduction: putting all the pieces together again. *FASEB J.*, **20**, 811–827.

Kalluri,R. (2009) EMT: when epithelial cells decide to become mesenchymal-like cells. *J. Clin. Invest.*, **119**, 1417–1419.

Kalluri,R. and Weinberg,R.A. (2009) The basics of epithelial-mesenchymal transition. *J. Clin. Invest.*, **119**, 1420–1428.

Kanehisa,M. and Goto,S. (2000) KEGG: kyoto encyclopedia of genes and genomes. *Nucleic Acids Res.*, **28**, 27–30.

Kroepil,F. *et al.* (2012) Down-regulation of CDH1 is associated with expression of SNAI1 in colorectal adenomas. *PloS ONE*, **7**, e46665.

Langevin,H.M. *et al.* (2006) Subcutaneous tissue fibroblast cytoskeletal remodeling induced by acupuncture: evidence for a mechanotransduction-based mechanism. *J. Cell. Physiol.*, **207**, 767–774.

Lee,K. and Nelson,C.M. (2012) New insights into the regulation of epithelial-mesenchymal transition and tissue fibrosis. *Int. Rev. Cell Mol. Biol.*, **294**, 171–221.

Lu,H. *et al.* (2006) Inflammation, a key event in cancer development. *Mol. Cancer Res. MCR*, **4**, 221–233.

Machacek,M. *et al.* (2009) Coordination of Rho GTPase activities during cell protrusion. *Nature*, **461**, 99–103.

Marshall,K.L. and Lumpkin,E.A. (2012) The molecular basis of mechanosensory transduction. *Adv. Exp. Med. Biol.*, **739**, 142–155.

Mendez,M.G. and Janmey,P.A. (2012) Transcription factor regulation by mechanical stress. *Int. J. Biochem. Cell Biol.*, **44**, 728–732.

Mi,H. *et al.* (2005) The PANTHER database of protein families, subfamilies, functions and pathways. *Nucleic Acids Res.*, **33**, D284–D288.

Parsons,J.T. *et al.* (2010) Cell adhesion: integrating cytoskeletal dynamics and cellular tension. *Nat. Rev. Mol. Cell Biol.*, **11**, 633–643.

Pecchi,E. *et al.* (2014) Induction of nerve growth factor expression and release by mechanical and inflammatory stimuli in chondrocytes: possible involvement in osteoarthritis pain. *Arthritis Res. Ther.*, **16**, R16.

Ponti,A. *et al.* (2004) Two distinct actin networks drive the protrusion of migrating cells. *Science*, **305**, 1782–1786.

Posern,G. and Treisman,R. (2006) Actin' together: serum response factor, its cofactors and the link to signal transduction. *Trends Cell Biol.*, **16**, 588–596.

Roussos,E.T. *et al.* (2010) AACR special conference on epithelial-mesenchymal transition and cancer progression and treatment. *Cancer Res.*, **70**, 7360–7364.

Ruths,D. *et al.* (2008) The signaling Petri net-based simulator: a non-parametric strategy for characterizing the dynamics of cell-specific signaling networks. *PLoS Comput. Biol.*, **4**, e1000005.

Schäfer,M. and Werner,S. (2008) Cancer as an overhealing wound: an old hypothesis revisited. *Nat. Rev. Mol. Cell Biol.*, **9**, 628–638.

Schwarz,U.S. and Gardel,M.L. (2012) United we stand: integrating the actin cytoskeleton and cell-matrix adhesions in cellular mechanotransduction. *J. Cell Sci.*, **125**, 3051–3060.

Shen,R. *et al.* (2009) Integrative clustering of multiple genomic data types using a joint latent variable model with application to breast and lung cancer subtype analysis. *Bioinformatics*, **25**, 2906–2912.

Smoot,M.E. *et al.* (2011) Cytoscape 2.8: new features for data integration and network visualization. *Bioinformatics*, **27**, 431–432.

Somogyi,K. and Rørth,P. (2004) Evidence for tension-based regulation of Drosophila MAL and SRF during invasive cell migration. *Dev. Cell*, **7**, 85–93.

Theocharidis,A. *et al.* (2009) Network visualization and analysis of gene expression data using BioLayout Express(3D). *Nat. Protoc.*, **4**, 1535–1550.

Theriot,J.A. and Mitchison,T.J. (1991) Actin microfilament dynamics in locomoting cells. *Nature*, **352**, 126–131.

Van Damme,J. *et al.* (1985) Homogeneous interferon-inducing 22K factor is related to endogenous pyrogen and interleukin-1. *Nature*, **314**, 266–268.

Wall,M.E. and Banes,A.J. (2005) Early responses to mechanical load in tendon: role for calcium signaling, gap junctions and intercellular communication. *J. Musculoskelet. Neuronal Interact.*, **5**, 70–84.

Wong,V.W. *et al.* (2012). Soft tissue mechanotransduction in wound healing and fibrosis. *Semin. Cell Dev. Biol.*, **23**, 981–986.

Wu,G. *et al.* (2010) A comprehensive molecular interaction map for rheumatoid arthritis. *PLoS ONE*, **5**, e10137.

Wynn,T.A. (2008) Cellular and molecular mechanisms of fibrosis. *J. Pathol.*, **214**, 199–210.

Zebda,N. *et al.* (2012) Focal adhesion kinase regulation of mechanotransduction and its impact on endothelial cell functions. *Microvasc. Res.*, **83**, 71–81.

Zhang,H. and Labouesse,M. (2012) Signalling through mechanical inputs: a coordinated process. *J. Cell Sci.*, **125**, 3039–3049.